

Microstructure and Mechanical Properties of a Polyethylene/ Polydimethylsiloxane Composite Prepared Using Supercritical Carbon Dioxide

Rui Zhu,¹ Toru Hoshi,^{2,3} Yoshio Muroga,^{2,3} Toshiki Hagiwara,² Shoichiro Yano,^{2,3}
Takashi Sawaguchi^{2,3}

¹Department of Materials and Applied Chemistry, Graduate School of Science and Technology, Nihon University, Chiyoda-ku, Tokyo 101-8308, Japan

²Department of Materials and Applied Chemistry, College of Science and Technology, Nihon University, Chiyoda-ku, Tokyo 101-8308, Japan

³Research Institute of Science and Technology, College of Science and Technology, Nihon University, Chiyoda-ku, Tokyo 101-8308, Japan

Correspondence to: R. Zhu (E-mail: iamzhurui814@yahoo.co.jp) or T. Sawaguchi (E-mail: sawaguchi.takashi@nihon-u.ac.jp)

ABSTRACT: A polymer composite of polyethylene (PE) and polydimethylsiloxane (PDMS) was prepared using supercritical carbon dioxide despite the two polymers usually being immiscible and possessing a phase-separated morphology. This article reports in detail the preparation, microstructure, crystallinity, and mechanical properties of the resulting PE/PDMS composite. The formation mechanism of the PE/PDMS composite consisted of supercritical impregnation of an octamethylcyclotetrasiloxane (D4) monomer and an initiator into a PE substrate followed by *in situ* polymerization within the substrate. Differential scanning calorimetry, wide-angle X-ray diffraction, and small-angle X-ray scattering measurements showed that PE and PDMS were blended at the nanometer level. The PDMS generated in the amorphous region of PE did not affect its crystallinity. Dynamic viscoelastic analyses and tensile tests were used to measure the mechanical properties of the composites including storage and Young's modulus, fracture stress, and strain. These properties were found to depend on the composition of the composite. © 2012 Wiley Periodicals, Inc. *J. Appl. Polym. Sci.* 000: 000–000, 2012

KEYWORDS: polyethylene; polysiloxanes; composites; microstructure; mechanical properties

Received 1 December 2011; accepted 5 February 2012; published online 00 Month 2012

DOI: 10.1002/app.37541

INTRODUCTION

Recently, a great deal of attention has been paid to supercritical carbon dioxide (scCO₂) as a solvent for small molecules¹ and/or swelling agent for polymer processing.^{2,3} However, it is a very poor solvent for most polymers even under extremely high pressures.⁴ The density of supercritical fluids (SCFs), and thus their solvent strength, is tunable from gas- to liquid-like by changing pressure and temperature. This provides the ability to control the degree of swelling of polymers as well as the partitioning of small molecules penetrating between swollen polymer and fluid phases.^{5,6} The low viscosity and near-zero surface tension of SCFs allow for rapid mass transfer into a swollen polymer. scCO₂ has been used to impregnate polymers with different additives. Because CO₂ is a gas under ambient conditions, the removal and recovery of solvent from final products are extremely facile.

Using scCO₂ as a swelling agent, Watkins and McCarthy developed a synthetic method to produce new polymer composites.⁷ Both the monomer and initiator were dissolved in scCO₂, impregnated into the polymer substrate, and subsequently polymerized. Using this method, we have already succeeded in obtaining microphase-separated polymer composites of polyethylene (PE)/poly(vinyl acetate) (PVAc) and polypropylene (PP)/poly(methyl methacrylate) (PMMA), even though these polymers are immiscible and cannot be obtained using conventional methods.^{8,9} The PE/PVAc composite features a biocompatible surface and can be used to fabricate medical devices. The PP/PMMA composite was blended at the nanometer level, and thus, favorable mechanical properties are expected. Polystyrene (PS) composites of semicrystalline and glassy polymer substrates such as PE, bisphenol-A polycarbonate, poly(oxyethylene),

© 2012 Wiley Periodicals, Inc.

nylon 66, poly(4-methyl-1-pentene), and poly(chlorotrifluoroethylene) have also been successfully synthesized.^{7,10,11} Kung et al. reported that mechanical properties such as Young's modulus and the yield stress of high-density polyethylene (HDPE)/PS composites obtained using scCO_2 could be controlled by composition.¹² In addition, they showed that the mechanical properties of a HDPE/PS composite prepared using scCO_2 were superior to a HDPE/PS blend prepared using the conventional melt-mixing process. Ultra-high molecular weight polyethylene (UHMWPE)/methacrylate polymer composites prepared with various hydrophobic methacrylate monomers featuring alkyl side chains of varying lengths instead of styrene, and the controlled preparation of copolymer blends of alkyl methacrylates within an UHMWPE substrate have also been reported.^{13–15} UHMWPE was also successfully blended with biodegradable polymers including polycaprolactone.¹⁶ Moreover, semi-interpenetrating polymer networks of UHMWPE with PMMA-co-poly(ethylene glycol) dimethacrylate were prepared via scCO_2 -facilitated impregnation of methyl methacrylate and ethylene glycol dimethacrylate monomers into UHMWPE.¹⁷ The mechanical properties of polymer composites prepared using scCO_2 can be controlled through the combination of substrate and monomer.

PE is considered the most important and widely used thermoplastic because of its low cost, good processability, and wide range of technical properties. However, PE has some disadvantages such as low surface energy, lack of chemical functionality, difficulty in dyeing and poor compatibility with synthetic polar polymers. Moreover, when a polymer composite of PE and other polymers is prepared, phase separation occurs, and a macro domain structure is formed because of the crystal growth of PE from the melt or soluble state.¹⁸

Polydimethylsiloxane (PDMS) is an inorganic polymer possessing good thermal stability and dielectric properties, and it is an excellent flame retardant. It also exhibits extremely low glass transition temperature, high flexibility, and hydrophobic surface properties.^{19–22} These properties make PDMS suitable for use in different industries.^{23–27} Blending PE and PDMS should allow new and useful polymer products that possess specific properties from the base polymers to be fabricated.

Several studies have investigated the phase behavior of PE/PDMS composites.^{28,29} These studies reported that PE and PDMS are immiscible because of their structural dissimilarity, lack of specific interaction, and differences between their surface energies. Kiran et al. prepared a PE/PDMS composite by direct impregnation and blending of PE and PDMS in scCO_2 .³⁰ However, this method is limited by the molecular weight of PDMS, and requires high temperatures and pressures. In our previous article, we prepared a PE/PDMS composite by *in situ* polymerization of octamethylcyclotetrasiloxane (D4) using scCO_2 , and determined the surface properties and performed a depth analysis of the resulting PE/PDMS composite.³¹ The hydrophobicity of PE was improved by incorporating PDMS, and the structure of the PE/PDMS composite could be controlled by varying the polymerization time of D4. However, the microstructure and mechanical properties of PE/PDMS were not evaluated.

In this article, a PE/PDMS composite was fabricated using the technique described above. The reaction behavior of this system

and microstructure of PE/PDMS were examined. If the polymerization temperature is lower than the melting temperature of the PE crystal, the polymerization of D4 should be confined to the amorphous regions of the substrate. Consequently, we expect interesting mechanical properties from composites with such kinetically trapped microstructures. We report the results of a detailed study of the synthesis of these systems and their dynamic viscoelasticity, Young's modulus, fracture stress and strain. In addition, we examine how the addition of PDMS to PE alters the mechanical properties of PE/PDMS composites.

EXPERIMENTAL

Materials

A linear low-density PE substrate was prepared from a commercial pellet ($M_n = 7.2 \times 10^4$, $M_w/M_n = 3.3$, Mitsui Chemical, Tokyo, Japan) by hot pressing at 170°C. The substrate was cut into pieces with dimensions of $20 \times 20 \times 0.5 \text{ mm}^3$, extracted with chloroform for 24 h in a Soxhlet extractor, and dried *in vacuo* at room temperature. D4, hexamethyldisiloxane and sulfuric acid were purchased from Tokyo Chemical Industry, Japan; Acros Organics, France; and Kanto Chemical, Tokyo, Japan, respectively, and used without further purification. Carbon dioxide (CO_2) with a purity of 99.5% was provided by Tomoe Shokai, Tokyo, Japan, and used as received.

Preparation of the PE/PDMS Composite Using scCO_2

The apparatus used to prepare the PE/PDMS composite consisted of a 50 mL stainless steel vessel, magnetic stirrer, constant-temperature air bath (Model SCF-Sro, JASCO, Tokyo, Japan), thermocouple, and pressure gauge. The pressure gauge comprised a transducer (PTX1400, Druck, Tokyo, Japan) and an indicator, and had a precision of $\pm 0.2\%$ over the pressure range 0–40 MPa. The PE substrate, D4 (5 g), hexamethyldisiloxane (0.006 g) as a chain transfer agent, and sulfuric acid (one drop: 0.02 g) as an initiator were placed in the vessel and sealed. Air in the vessel was replaced by CO_2 at atmospheric pressure. After the system reached thermal equilibrium (35°C), the vessel was pressurized to a CO_2 pressure of 6.0 MPa using a CO_2 delivery pump (SCF-Get, JASCO, Japan). The PE substrate was soaked in subcritical CO_2 for 1 h. The vessel was then repressurized up to 6.0 MPa (to compensate for the drop in pressure caused by dissolution of the monomer and initiator) and heated to 80°C for a specific time. After completion of the reaction, the vessel was cooled to 10°C in an ice bath and gradually released to ambient pressure. The PE/PDMS composite was dried *in vacuo* at room temperature after extraction with chloroform for 24 h at 50°C using a Soxhlet extractor to remove unreacted reagents and the PDMS generated on the surface of the PE/PDMS composite. The PDMS that generated outside of PE was dissolved in chloroform. Then the solution was rotary evaporated to isolate the PDMS.

Characterization

Gravimetric Analysis. Gravimetric data were obtained by the following equation:

$$\text{Mass gain (wt\%)} = \frac{W_t - W_0}{W_0} \times 100 \quad (1)$$

where W_0 is the initial weight of the PE substrate and W_t is the weight of the PE/PDMS composite sheet after drying. The

measurement accuracy was $\pm 0.2\%$. The reported weight of the sample was the mean value of five repeat measurements.

Differential Scanning Calorimetry. The thermal behavior of the composite was measured using differential scanning calorimetry (DSC) (Seiko Instruments, DSC6100, Japan). The sample (2–3 mg) was packed into aluminum DSC sample pans with the lid tightly crimped. Measurements were taken between -100 and 200°C at a scan rate of $10^\circ\text{C}/\text{min}$ under a flow of nitrogen gas. The degree of crystallinity was determined using a standard heat of fusion value of 293 J/g .³²

Wide-Angle X-ray Diffraction. Wide-angle X-ray diffraction (WAXRD) experiments were performed at 20°C using a Panalytical X'Pert Pro diffractometer (The Netherlands). Cu $K\alpha$ radiation (wavelength, $\lambda = 0.154\text{ nm}$) was generated at 45 kV and 40 mA . All samples were scanned at a rate of $3^\circ/\text{min}$ between 10° and 50° in transmission mode. The crystallinity was determined by assuming that the total diffraction within a certain region of reciprocal space was independent of the state of aggregation of the material. The crystallinity, X_c , expressed as the mass fraction of the crystalline component, is then given as:

$$X_c = \frac{A_c}{A_c + A_a} \quad (2)$$

where A_a is the area under the peaks corresponding to the amorphous region and A_c is the area remaining under the crystalline peaks.³³

Small-Angle X-ray Scattering. The microstructure of obtained PE/PDMS composite was investigated by small-angle X-ray scattering (SAXS). The X-ray beam was from synchrotron radiation: beam line BL-10C at the High Energy Accelerator Research Organization (KEK), Tsukuba, Japan (Photon Factory).³⁴ The storage ring was operated at an energy of 2.5 GeV with a ring current of $300\text{--}450\text{ mA}$. SAXS employs point focusing optics with a double flat monochromator followed by a bent cylindrical mirror. The intensity of the incident beam with a wavelength 1.488 \AA was monitored in an ionization chamber to correct the minor decrease in the intensity of the primary beam during the measurement. The scattering intensity was detected with a one-dimensional position sensitive proportional counter (PSPC) with 512 channels, and the distance between the sample and the PSPC was about 2 m . The geometry was checked using chicken tendon collagen, which gives a set of sharp diffractions corresponding to a Bragg spacing of 653 \AA .

The scattering intensity, $I(q)$, was corrected for background scattering after a smoothing procedure. Smoothing of the experimental scattering data was performed using a binomial calculation. The scattering intensity from thermal fluctuations was subtracted from the SAXS profile $I(q)$ by evaluating the slope of $I(q)q^4$ versus q^4 plots³⁵ at wide scattering vector q , where q is $(4\pi/\lambda) \sin \theta$, and λ and θ are the wavelength and scattering angle, respectively.

Mechanical Properties. The dynamic viscoelastic properties of the composite were measured in tensile mode using a dynamic viscoelastic analyzer (DVA-220, IT Keisoku Seigy Company, Japan) with a chuck distance of 10 mm and a frequency of

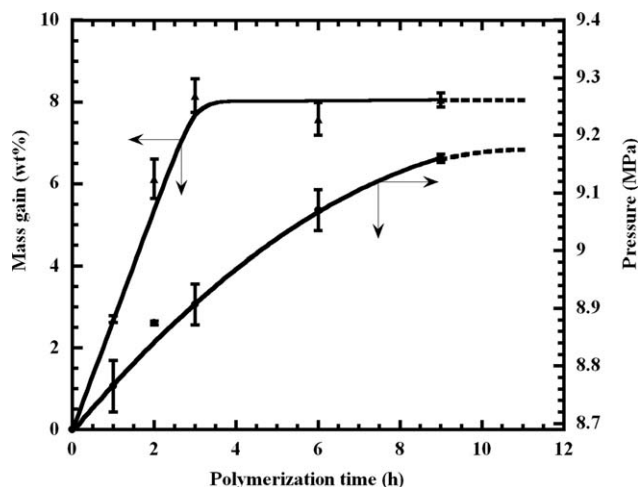


Figure 1. Effect of polymerization time on the mass gain of PDMS into PE substrate and the pressure after polymerization (triangles: mass gain; circles: pressure).

10 Hz . The storage modulus (E'), loss modulus (E'') and loss tangent ($\tan \delta$) were measured as a function of temperature using a heating rate of $5^\circ\text{C}/\text{min}$.

Tensile tests were carried out using a screw-driven tensile machine (IM-20ST, Intesco, Japan) with a grip interval of 10 mm . All samples were deformed at 20°C at a strain rate of $100\%/ \text{min}$.

RESULTS AND DISCUSSION

Gravimetric Analysis

Figure 1 shows the effect of polymerization time on the percentage mass gain of PDMS in the PE substrate and the pressure after polymerization. As expected, an obvious mass gain by successive addition was observed until 3 h , and then it remains almost constant. Under these conditions ($P < 10\text{ MPa}$, $T = 80^\circ\text{C}$), PDMS does not dissolve in scCO_2 .^{36,37} When PDMS is generated on the exterior of the PE substrate, the pressure increases so that the volume of the gas phase in the vessel decreases. The polymerization process can be divided into three stages. In the primary stage of polymerization (polymerization time $< 3\text{ h}$), the mass gain and pressure increase with polymerization time. Therefore, PDMS was polymerized both in the interior and exterior of the PE substrate. The formation mechanism of the PE/PDMS polymer composite is thought to be as follows (Figure 2): the monomer and initiator dissolve in scCO_2 and impregnate the amorphous interlamellar regions of the PE substrate; after reaching the polymerization temperature, the monomer polymerizes within the amorphous interlamellar regions of the PE substrate. Polymerization of the monomer leads to an imbalance in the partition coefficient of the monomer within and outside the PE substrate. The monomer outside the PE substrate then permeates into the amorphous regions of the PE substrate, and polymerization continues. As a result, PE and PDMS were effectively blended at the nanometer level. In the secondary stage ($3\text{ h} < \text{polymerization time} < 10\text{ h}$), only the pressure increases as polymerization progresses. Therefore, PDMS is only polymerized outside the PE substrate. A possible

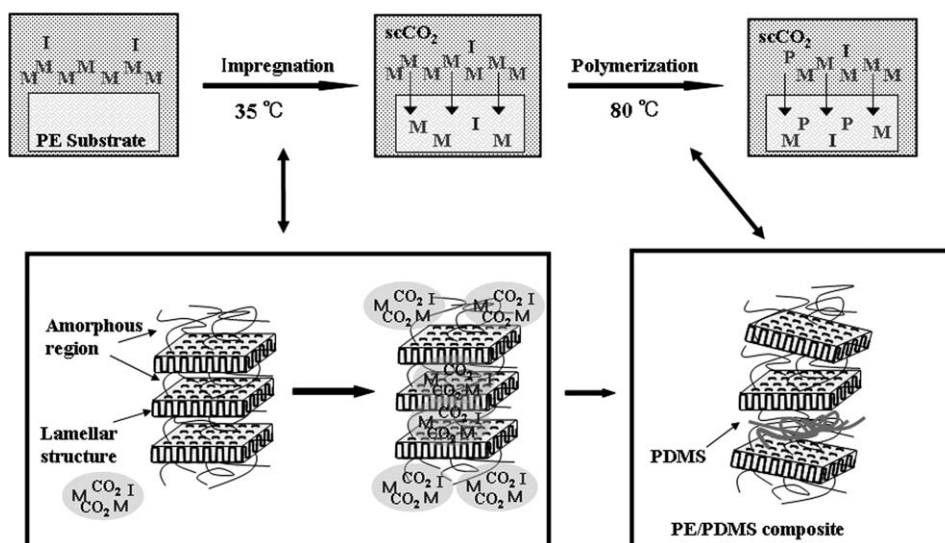


Figure 2. Formation mechanism of the PE/PDMS composite [M: monomer (D4) P: Polymer (PDMS) I: Initiator (H_2SO_4)].

reason for PDMS not being polymerized in the interior of the PE substrate is that the PDMS formed on the surface of the PE substrate prevents impregnation of the monomer and initiator. In the third stage (polymerization time > 10 h), the mass gain and pressure do not increase with polymerization time. This indicates that polymerization is complete.

Figure 3 shows the effect of polymerization time on monomer conversion inside and outside PE. Monomer conversion inside the PE substrate increases initially and reaches a plateau after 3 h, while monomer conversion outside PE becomes saturated after 10 h. This is consistent with the polymerization process being divided into three stages.

It is necessary to increase the mass gain of PDMS because it affects mechanical properties such as storage and Young's moduli, fracture stress and strain (described in "Mechanical properties" section). To increase the mass gain, the amount of monomer inside the PE substrate should be increased. This could be realized by changing the initial pressure or soaking time. It is considered that increasing the initial pressure will increase the solubility of the monomer in scCO_2 .^{38–41} The amount of impregnated low-molecular weight components also depends on the soaking time, where an equilibrium value is obtained after a certain time.⁴² The soaking time results in an equilibrium of the monomer concentration inside and outside the PE substrate. Thus, the concentration of polymer in the substrate can be further enhanced by changing the initial pressure and soaking time.

In addition, the impregnation of scCO_2 starts on the surface of the substrate and then gradually progresses to the inner substrate. The role of scCO_2 is then to dissolve D4 and H_2SO_4 and to carry the monomer and initiator into the amorphous regions of the PE substrate. The swelling kinetics of CO_2 in the polymer matrix depend on the temperature and pressure.^{43,44} Therefore, controlling the penetration depth of PDMS can be achieved by controlling the diffusion and solubility of scCO_2 according to temperature and pressure.

Characterization of PE/PDMS Composite

Figure 4 shows WXR patterns of the original PE, PE treated with scCO_2 , and PE/PDMS composites, which exhibit characteristic peaks of the (110) and (200) planes. The angular positions of the diffraction peaks of crystalline PE are almost identical in original PE, PE treated with scCO_2 , and PP/PDMS composites, indicating that the crystal forms do not change upon scCO_2 treatment or addition of PDMS. However, the amorphous region of the PE/PDMS composite increases as the mass gain of PDMS increases, which indicates that the overall crystallinity decreases as the mass gain of PDMS increases (Figure 5). The reduction in sample crystallinity is caused by dilution as a result of formation of PDMS in the amorphous regions of PE and the resultant increase in the size of these regions. The percentage crystallinity in PE, X_{PE} , was calculated as follows:

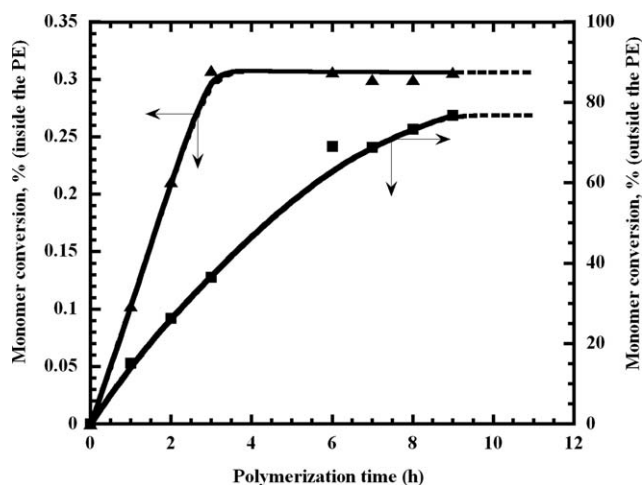


Figure 3. Effect of polymerization time on the monomer conversion inside and outside the PE (triangles: inside the PE; circles: outside the PE).

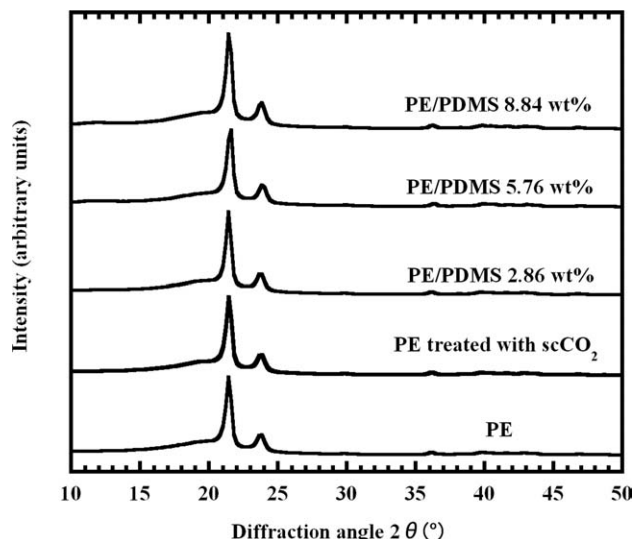


Figure 4. WAXD patterns of original PE, PE treated with scCO_2 and PE/PDMS composites.

$$X_{\text{PE}} (\%) = \frac{X_{\text{PE/PDMS}}}{W_{\text{PE}}} \quad (3)$$

where X_{PE} is the crystallinity of PE/PDMS composite that is assumed to be dependent only on the crystalline regions of PE, $X_{\text{PE/PDMS}}$ is the crystallinity of the entire PE/PDMS composite, and W_{PE} is the weight fraction of PE. X_{PE} does not change although $X_{\text{PE/PDMS}}$ decreases as the mass gain of PDMS increases. These results indicate that D4 polymerizes solely within the amorphous regions of PE.

Figure 6 shows DSC thermograms of the original PE, PE treated with scCO_2 , and PE/PDMS composite with a mass gain of 9.09 wt %. The DSC thermogram of PE treated with scCO_2 changed without increasing the degree of crystallinity compared with the original PE. This result implies that the swelling of scCO_2 at a

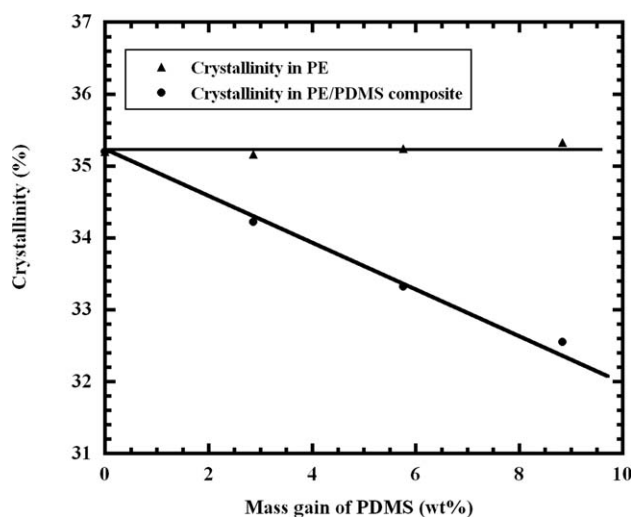


Figure 5. Relationship between crystallinity and mass gain in PDMS.

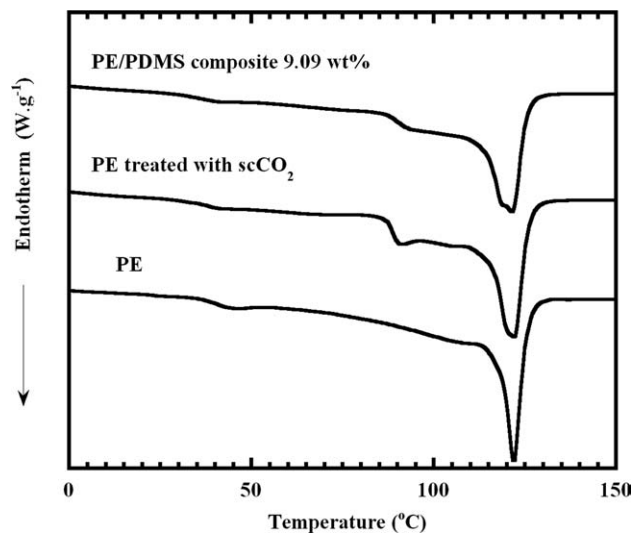


Figure 6. DSC thermograms of PE, PE-treated with scCO_2 , and PE/PDMS composite (mass gain: 9.09 wt %).

treatment temperature of 80°C produces the same effect as isothermal crystallization.⁴⁵ In the PE/PDMS composite, a strong PE melting endotherm was observed. The melting endotherm reveals that the composite does not affect the crystalline region of the PE substrate. The degree of crystallinity of the original PE and PE/PDMS composite was found to be 35.2 and 32.5 wt %, respectively. The reduction in sample crystallinity is entirely because of dilution by the addition of PDMS to the amorphous PE regions. The total amount of crystalline region of PE remained unchanged. In addition, it was found that the DSC traces of the PE treated with scCO_2 and PE/PDMS composite exhibited a second low T_m endothermic peak as well as from the main crystalline melting peak. This means that small crystals were present in the PE treated with scCO_2 and PE/PDMS composite.

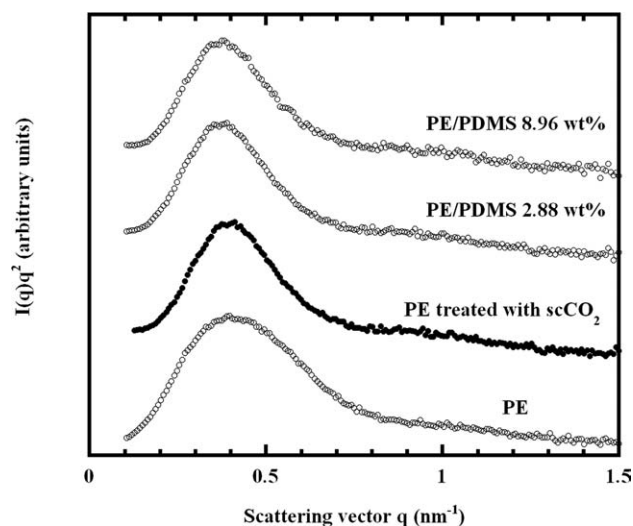


Figure 7. Lorentz-corrected SAXS profiles of original PE, PE treated with scCO_2 , and PE/PDMS composites.

Microstructural Analysis of the PE/PDMS Composite

The effect of formation of PDMS in the amorphous regions of the PE substrate on its microstructure was investigated by SAXS. Figure 7 shows the Lorentz-corrected SAXS profiles of original PE, PE treated with scCO_2 , and PE/PDMS composites. In the spectrum of original PE, the scattering vector q of the peak top was 0.397 nm^{-1} (calculated using a Bragg spacing of 15.8 nm). This peak was caused by the long period of the lamellar structure.^{46,47} The positions of the peak in the PE treated with scCO_2 was the same as that in the original PE. However, the peak of the PE treated with scCO_2 was sharper. This implies that a small crystal of PE grew, which is consistent with the DSC results. In the PE/PDMS composite, the peak from long period shifted slightly toward lower q . This change was not observed for the CO_2 -treated PE. The extent of this change depended on the mass gain of PDMS. This result is consistent with the generation of small-angle scattering from extensive disruption of the crystalline lamellar upon incorporation of PDMS into the polymer composites. The results of DSC and WAXD measurements indicate that the total amount of crystalline region of PE and the crystal structure of PE do not change. Therefore, these SAXS measurements indicate that PDMS formed in the amorphous regions between the crystalline lamellar of PE, and that PE and PDMS were blended at the nanometer level.

Mechanical Properties

The dynamic viscoelastic behavior of PE and the PE/PDMS composites is represented as a function of temperature in Figure 8. At a lower temperature than the glass transition temperature of PDMS ($T_{g,\text{PDMS}}$) at $\sim 123^\circ\text{C}$,⁴⁸ the storage modulus of the PE/PDMS composite was larger than that of PE. Furthermore, at temperatures higher than $T_{g,\text{PDMS}}$, the storage modulus of the PE/PDMS composite was smaller than that of PE. This change in the storage modulus of the PE/PDMS composite depends on the mass gain. This occurs because, at temperatures lower than $T_{g,\text{PDMS}}$, the chain mobility of the amorphous

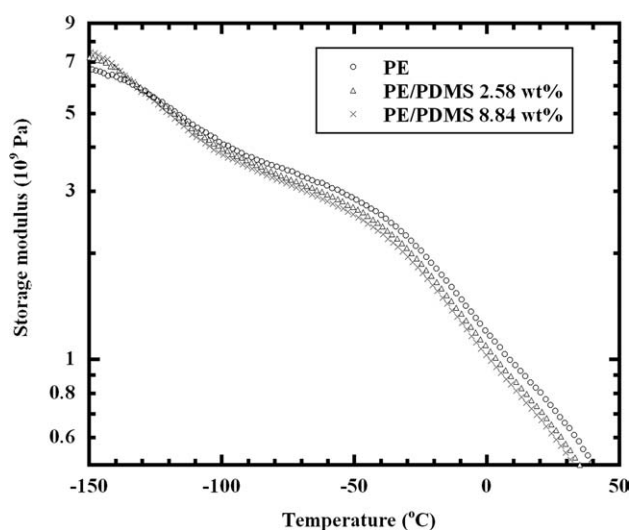


Figure 8. Temperature dispersion curves of the storage modulus (E') for original PE and PE/PDMS composites.

Table I. Results of the Tensile Tests at 20°C

Sample name	Young's modulus (MPa)	Fracture stress (MPa)	Fracture strain (%)
PE	130	9	922
PE/PDMS (5.76 wt %)	70	7.6	836
PE/PDMS (8.84 wt %)	57	5.6	738

regions of PE is retarded by the glassy PDMS that is generated in the amorphous regions. The decreased mobility of the amorphous PE chains increases the storage modulus of the PE/PDMS composite so that is larger than that of PE. Above $T_{g,\text{PDMS}}$, the amorphous regions of the PE/PDMS composite increase more than that of PE because of the micro-Brownian motion of PDMS.

Table 1 lists the results of tensile testing at 20°C above $T_{g,\text{PDMS}}$. Because the amorphous regions of the PE/PDMS composite increase more than that of PE because of the micro-Brownian motion of PDMS at 20°C , the Young's modulus, fracture stress and strain of the PE/PDMS composite decrease as the mass gain of PDMS increases. This is consistent with the results of DVA. Therefore, the nanometer-sized PDMS generated in the amorphous regions significantly affects the mechanical properties of the PE/PDMS composite, which can be controlled through the mass gain of PDMS.

CONCLUSION

We prepared PE/PDMS composites by *in situ* cationic polymerization using scCO_2 . PDMS formed in the amorphous regions between the crystalline lamellar of PE, which did not affect its crystallinity. PE and PDMS were blended at the nanometer level. The presence of PDMS in the amorphous regions significantly affects the viscoelasticity and mechanical properties of the PE/PDMS composite. The storage modulus of the PE/PDMS composite changes at $T_{g,\text{PDMS}}$. Below $T_{g,\text{PDMS}}$, the chain mobility of the amorphous regions of PE is retarded by the glassy PDMS, and the storage modulus of the PE/PDMS composite is larger than that of PE. Above $T_{g,\text{PDMS}}$, the amorphous regions of the PE/PDMS composite increase more than that of PE because of the micro-Brownian motion of PDMS, so the storage modulus of the PE/PDMS composite is smaller than that of PE. Mechanical properties such as Young's modulus, tensile strength, and elongation at break of the PE/PDMS composite can be controlled by the mass gain of PDMS. Also, PDMS formed on the surface of PE improved its hydrophobicity. Thus, new materials with desirable mechanical and surface properties can be formed by tuning conditions such as the ratio of blending polymer, and the type of polyolefin and blending polymer.

REFERENCES

1. Kamiya, Y.; Mizoguchi, K.; Terada, K.; Fujiwara, Y.; Wang, J. *Macromolecules* **1998**, *31*, 472.
2. Cooper, A. I. *J. Mater. Chem.* **2000**, *10*, 207.

3. Kendall, J. L.; Canelas, D. A.; Young, J. L.; DeSimone, J. M. *Chem. Rev.* **1999**, *99*, 543.
4. Rindfleisch, F.; DiNoia, T. P.; McHugh, M. A. *J. Phys. Chem.* **1996**, *100*, 15581.
5. Shim, J. J.; Johnston, K. P. *AIChE J.* **1989**, *35*, 1097.
6. Shim, J. J.; Johnston, K. P. *AIChE J.* **1991**, *37*, 607.
7. Watkins, J. J.; McCarthy, T. *Macromolecules* **1994**, *27*, 4845.
8. Hoshi, T.; Sawaguchi, T.; Konno, T.; Takai, M.; Ishihara, K. *Polymer* **2007**, *48*, 1573.
9. Zhu, R.; Hoshi, T.; Chishima, Y.; Muroga, Y.; Hagiwara, T.; Yano, S.; Sawaguchi, T. *Macromolecules* **2011**, *44*, 6103.
10. Li, D.; Liu, Z.; Han, B.; Song, L.; Yang, G.; Jiang, T. *Polymer* **2002**, *43*, 5363.
11. Watkins, J. J.; McCarthy, T. J. *Macromolecules* **1995**, *28*, 4067.
12. Kung, E.; Lesser, A. J.; McCarthy, T. J. *Macromolecules* **1998**, *31*, 4160.
13. Zhang, J.; Busby, A. J.; Roberts, C. J.; Chen, X.; Davies, M. C.; Tendler, S. J. B.; Howdle, S. M. *Macromolecules* **2002**, *35*, 8869.
14. Busby, A. J.; Zhang, J.; Naylor, A.; Roberts, C. J.; Davies, M. C.; Tendler, S. J. B.; Howdle, S. M. *J. Mater. Chem.* **2003**, *13*, 2838.
15. Naylor, A.; Howdle, S. M. *J. Mater. Chem.* **2005**, *15*, 5037.
16. Busby, A. J.; Zhang, J.; Roberts, C. J.; Lester, E.; Howdle, S. M. *Adv. Mater.* **2005**, *17*, 364.
17. Naylor, A.; Timashev, P. S.; Solov'eva, A. B.; Erina, N. A.; Kotova, S.; Busby, A. J.; Popov, V. K.; Howdle, S. M. *Adv. Mater.* **2008**, *20*, 575.
18. Akiyama, S.; Inoue, T.; Nishi, T. In *Polymer Blend*; CMC Publishing Company: Japan, **1981**; p 56–59.
19. Yilgor, I.; Steckle, J. W.; Yilgor, E.; Freelin, R.; Riffle, J. *J. Polym. Sci. Part A: Polym. Chem.* **1989**, *27*, 3673.
20. Riffle, J.; Yilgor, I.; Banthia, A.; Wilkes, G.; McGrath, J. *Org. Coat. Appl. Polym. Sci. Proc.* **1981**, *46*, 397.
21. Garin, S.; Lecamp, L.; Youssef, B.; Bunel, C. *Eur. Polym. J.* **1999**, *35*, 473.
22. Hou, S.; Chung, Y.; Chan, C.; Kuo, P. *Polymer* **2000**, *41*, 3263.
23. Qi, R.; Wang, Y.; Li, J.; Zhao, C.; Zhu, S. *J. Membr. Sci.* **2006**, *280*, 545.
24. Luo, C.; Meng, F.; Francis, A. *Microelectronics J.* **2006**, *37*, 1036.
25. Lehmann, R.; Miller, J.; Kozerski, G. *Chemosphere* **2000**, *41*, 743.
26. Jo, B.; Van, L.; Linda, M.; Motsegood, K.; Beebe, D. *J. Microelectromech. Syst.* **2000**, *9*, 76.
27. Polmanteer, K.; Chapman, H.; Lutz, M. *Rubber Chem. Technol.* **1985**, *58*, 965.
28. Chalykh, A.; Avdeyev, N. *Polym. Sci. USSR* **1985**, *27*, 2769.
29. Huglin, M.; Idris, I. *Eur. Polym. J.* **1985**, *21*, 9.
30. Bayraktar, Z.; Kiran, E. *J. Supercrit. Fluid* **2008**, *44*, 48.
31. Zhu, R.; Hoshi, T.; Sasaki, D.; Usui, R.; Hagiwara, T.; Yano, S.; Sawaguchi, T. *Polym. J.* **2010**, *42*, 562.
32. Runt, R. P. In *Encyclopedia of Polymer Science and Engineering*; Mark, H. F., Bikales, N. M., Overberger, C. G., Menges, G., Eds.; Wiley-Interscience: New York, **1986**; vol.4, p 482.
33. FlyantS, A. J.; Stanford, J. L. *Polymer* **1997**, *38*, 759.
34. Ueki, T.; Hiragi, Y.; Kataoka, M.; Inoko, Y.; Amemiya, Y.; Izumi, T.; Tagawa, H.; Muroga, Y. *Biophys. Chem.* **1985**, *23*, 115.
35. Koberstein, J. T.; Morra, B.; Stein, R. S. *J. Appl. Cryst.* **1980**, *13*, 34.
36. Bayraktar, Z.; Erdpagan, K. *J. Appl. Polym. Sci.* **2000**, *75*, 1397.
37. Xiong, Y.; Kiran, E. *Polymer* **1995**, *36*, 4817.
38. Kirby, C. F.; McHugh, M. A. *Chem. Rev.* **1999**, *99*, 565.
39. Sato, Y.; Fujiwara, K.; Takikawa, T.; Sumarno; Takishima, S.; Masuoka, H. *Fluid Phase Equilib.* **1999**, *162*, 261.
40. Berens, L. R.; Huvar, G. S.; Korsmeyer, R. W.; Kunig, F. W. *J. Appl. Polym. Sci.* **1992**, *46*, 231.
41. Li, D.; Liu, Z.; Han, B.; Song, L.; Yang, G.; Jiang, T. *Polymer* **2002**, *43*, 5363.
42. Li, D.; Han, B.; Liu, Z. *Macromol. Chem. Phys.* **2001**, *202*, 2187.
43. Nikitin, L. N.; Said-Galiyev, E. E.; Vinokur, R. A.; Khokhlov, A. R.; Gallyamov, M. O.; Schaumburg, K. *Macromolecules* **2002**, *35*, 934.
44. Royer, J. R.; DeSimone, J. M.; Khan, S. A. *Macromolecules* **1999**, *32*, 8965.
45. Schouterden, P.; Groeninckx, G.; Heijden, B.; Jansen, F. *Polymer* **1987**, *28*, 2099.
46. Ryan, A. J.; Bras, W.; Mant, G. R.; Derbyshire, G. E. *Polymer* **1994**, *35*, 4537.
47. Ryan, A. J.; Stanford, J. L.; Bras, W.; Nye, T. M. W. *Polymer* **1997**, *38*, 759.
48. Tiwari, A.; Nema, A. K.; Das, C. K.; Nema, S. K. *Thermochim. Acta.* **2004**, *417*, 133.